



Cite this: *RSC Adv.*, 2018, 8, 6075Received 5th December 2017  
Accepted 31st January 2018

DOI: 10.1039/c7ra13048a

rsc.li/rsc-advances

# Determination of berberine hydrochloride using a fluorimetric method with silica nanoparticles as a probe

Qing Liu,  Zhihai Xie,\* Tao Liu  and Jin Fan

The interaction of silica nanoparticles (SiO<sub>2</sub>NPs) with berberine hydrochloride (BRH) was studied in aqueous solution at pH 9.0 and room temperature by using fluorophotometry. Based on a significant enhancement of the fluorescence intensity of the SiO<sub>2</sub>NPs–BRH aggregates, a spectrofluorimetric method which was simple, sensitive and green was developed for the determination of BRH in aqueous solution. The linear range of the method was from 2.0–50.0 μg L<sup>-1</sup> with a detection limit of 0.73 μg L<sup>-1</sup>. There was no interference from the compounds normally used to formulate pharmaceutical tablets. The proposed method was applied to the determination of BRH in tablets with satisfactory results and good consistency with the results obtained by standard methods.

## 1. Introduction

Berberine hydrochloride (BRH, the molecular structure is shown in Fig. 1) is a significant natural isoquinoline alkaloid, which is a key active ingredient in traditional Chinese medicine. It is widely used as an antibacterial and anti-inflammatory drug in pharmaceutical products.<sup>1,2</sup> Recently, there has been a growing interest in the pharmaceutical activities of BRH toward infectious diseases, cardiovascular disorders, diabetes, and cancer.<sup>3–5</sup> Due to the bioactivity and wide potential applications of BRH, many analytical methods have been reported for the its determination, including spectrophotometry,<sup>6–8</sup> resonance light scattering spectrometry (RLS),<sup>9,10</sup> chemiluminescence,<sup>11</sup> high performance liquid chromatography (HPLC),<sup>12,13</sup> capillary electrophoresis,<sup>14</sup> and electrochemical analysis.<sup>15,16</sup> Another analytical method gaining importance is fluorophotometry, which is characterized by its high selectivity and sensitivity, simple setup, and convenient operation. Fluorophotometry has been widely applied for the determination of different analytes, including inorganic ions, organic compounds, biomacromolecules, and pharmaceuticals.<sup>17–20</sup> Furthermore, sensitive fluorophotometry has been reported with metal nanoparticles as probes for the determination of organic compounds and BRH,<sup>21–24</sup> and receptor molecules such as cyclodextrin,<sup>25,26</sup> calixarenes,<sup>27</sup> and cucurbituril<sup>28</sup> have also been used for the determination of BRH by fluorophotometry. These molecules are capable of interacting with the BRH molecules through noncovalent intermolecular forces or cavity

encapsulation to form aggregations (or supramolecular complexes). The formation of the aggregation often affects the enhancements or perturbations of the photophysical and photochemical properties of the included guest molecules.<sup>29</sup>

In recent years, silica nanoparticles (SiO<sub>2</sub>NPs) have attracted remarkable interest for biomedical applications because of their special physicochemical properties, such as good solid dispersions, relatively large specific surface areas and biocompatibility, low cost, ease of production, and lack of toxicity. Pure and dye-doped SiO<sub>2</sub>NPs were prepared, and their surfaces were modified with enzymes and biocompatible chemical reagents that allow them to function as biosensors and biomarkers.<sup>30–33</sup> Sensitive and selective fluorescent aptasensors based on SiO<sub>2</sub>-NPs have been investigated for the determination of bio-macromolecules or drugs.<sup>34,35</sup> Moreover, Fan<sup>36</sup> reported the use of SiO<sub>2</sub>NPs as a probe for the determination of methylene blue by RLS technique. Nevertheless, the determination of BRH by fluorophotometry with SiO<sub>2</sub>NPs as a probe has not been reported.

In the present study, a marked increase was found in the fluorescence intensity of BRH in aqueous media with SiO<sub>2</sub>NPs. Therefore, a simple, novel, and green method for the detection of BRH in aqueous solution was developed by fluorophotometry

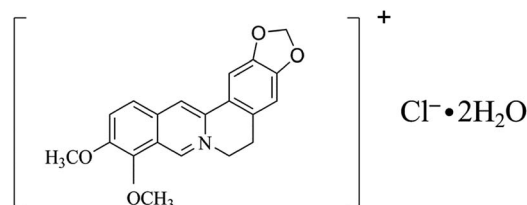


Fig. 1 The chemical structure of berberine hydrochloride.

Key Laboratory of Synthetic & Natural Functional Molecular Chemistry of the Ministry of Education, College of Chemistry & Material Science, Northwest University, No. 1 Xuefu Road, Xi'an, Shaanxi, 710127, China. E-mail: xiezhihai8@163.com; Fax: +86 029-81535026; Tel: +86 029-81535026



with SiO<sub>2</sub>NPs as a probe. In addition, the optimal factors for the determination of BRH were investigated, and the related mechanisms were also considered. This method was applied for the analysis of practical samples with respectable results.

## 2. Experimental

### 2.1. Reagents

BRH was purchased from Aladdin Chemical Reagent (Los Angeles, USA) and was used to prepare a 100.0 mg L<sup>-1</sup> stock solution. The working solutions were prepared by diluting the stock solution to 100.0 μg L<sup>-1</sup>. SiO<sub>2</sub>NPs (CQ380) were obtained from Emeishan Changqing Chemical New Material Co., Ltd. (China). Acetic acid, boric acid, phosphoric acid, and sodium hydroxide were supplied from the Xi'an Chemical Reagent Factory (Xi'an, China). A Britton–Robinson (BR) buffer solution was prepared by mixing 0.04 mol L<sup>-1</sup> acetic acid, 0.04 mol L<sup>-1</sup> boric acid, 0.04 mol L<sup>-1</sup> phosphoric acid, and 0.2 mol L<sup>-1</sup> sodium hydroxide solution in specific proportions. All chemicals used in the experiments were of analytical grade and used without further purification. Deionized water was used for preparing all samples and solutions.

### 2.2. Apparatus

The instruments used in this study were as follows: F-4500 spectrofluorophotometer (Hitachi, Japan); UV-1700 spectrophotometer (Shimadzu, Japan); H-600 transmission electron microscope (Hitachi, Japan); DB-525 Zeta Potential Analyzer (Brookhaven, USA); pHs-3C digital pH meter (Shanghai Lei Ci Device Works, China) with a glass electrode (Model E-201-C); and magnetic stirrer (Gongyi Yuhua Instrument Factory, China).

### 2.3. Preparation of SiO<sub>2</sub>NPs dispersion

Exactly 0.10 g of SiO<sub>2</sub>NPs was weighed out and added into 200.0 mL of deionized water under vigorous stirring for 10 min, and then the mixture was placed in an ultrasonic bath for 30 min at room temperature to completely disperse the SiO<sub>2</sub>-NPs. The concentration of the dispersion was 0.05%.

### 2.4. Preparation of samples

The sugar coating was carefully removed from 10 tablets and the contents were carefully pulverized. The powders were then thoroughly mixed. A portion of the mixed powders was accurately weighed and placed in a 100 mL volumetric flask. The powder was dissolved by addition of deionized water up to the mark and sonication for 10 min, and the solution was then filtered. The first 30 mL of the filtrate were discarded, a portion of the remaining filtered sample solution was diluted to the mark in a 100 mL volumetric flask, and this solution was analyzed according to the general procedure.

### 2.5. General procedure

The general procedure for determination of BRH is as follows: 0.8 mL of 0.05% SiO<sub>2</sub>NPs dispersion, 0.5 mL of BR buffer solution (pH 9.0), and a certain amount of BRH working

solution were added into a 10.0 mL volumetric flask, diluted to the mark with deionized water, and sonicated for 2 min. The resulting solution was left at room temperature for 30 min, and then the fluorescence intensity was measured at 540 nm with an excitation wavelength of 355 nm. The enhanced fluorescence intensities of the solutions were calculated by the following equation:  $\Delta I_F = I_F - I_{F0}$  (in which  $I_F$  and  $I_{F0}$  are the fluorescence intensities of the SiO<sub>2</sub>NPs in the presence and absence of BRH). All experiments were conducted at room temperature.

## 3. Results and discussion

### 3.1. Absorption spectra

The absorption spectra of BRH and the SiO<sub>2</sub>NPs–BRH aggregates are shown in Fig. 2. The absorbance of the solution gradually decreased and the absorption spectrum shifted toward longer wavelength (2–5 nm) with addition of SiO<sub>2</sub>NPs, as well as there were three obvious isobestic points (354 nm, 389 nm, 435 nm). This corresponds to the absorption of aggregates which is clearly different from unaggregated. In addition, the excitation spectrum at 450 nm was also observed except for 355 nm (Fig. 3A). The phenomena might be because the positive charge of BRH causes it to be adsorbed on the surface of the SiO<sub>2</sub>NPs to form SiO<sub>2</sub>NPs–BRH aggregates.<sup>37</sup>

### 3.2. Excitation and emission spectra

The excitation and emission spectra were measured according to the general procedure. The results are shown in Fig. 3. The excitation wavelengths were located at 355 and 450 nm, and the emission wavelengths were at 540 nm. The fluorescence intensities of the BRH and SiO<sub>2</sub>NPs on their own were very small at 540 nm in aqueous solution. However, when SiO<sub>2</sub>NPs was added to the aqueous solution of BRH, the fluorescence intensity was significantly enhanced. Because BRH molecules were bound to the surfaces of the SiO<sub>2</sub>NPs and protected as SiO<sub>2</sub>NPs–BRH aggregates, the fluorescence intensity increased.

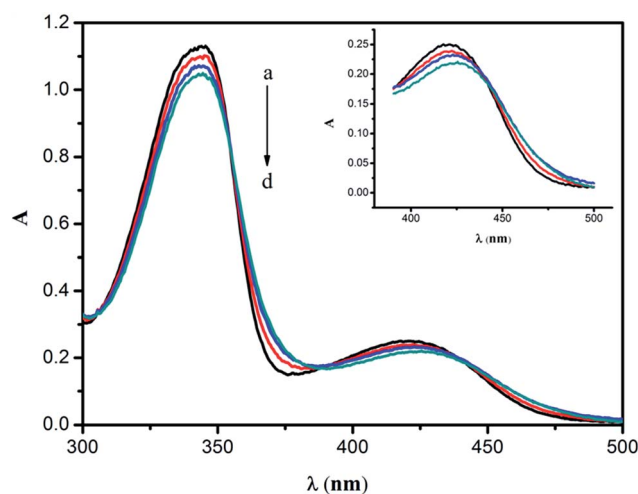


Fig. 2 Absorption spectra. Conditions: (a) BRH, 20 mg L<sup>-1</sup>; (b–d) a + SiO<sub>2</sub>NPs (0.01, 0.02, and 0.03%); pH 9.0.



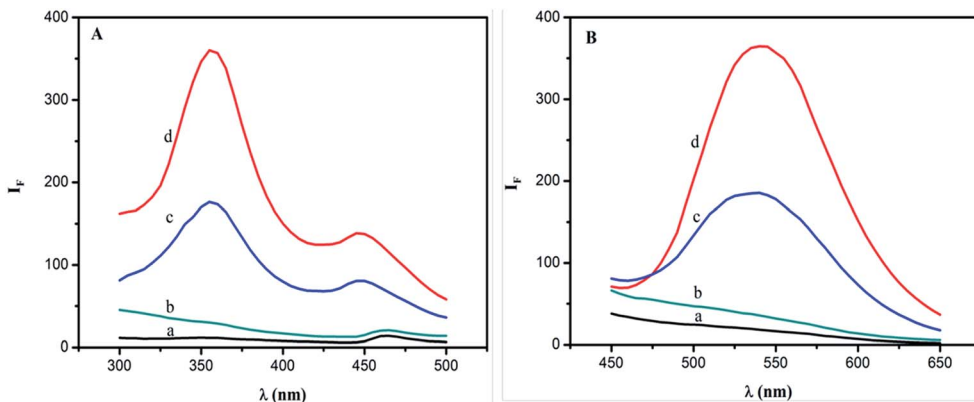


Fig. 3 Excitation (A) and emission (B) spectra. Conditions: (a) BRH,  $50 \mu\text{g L}^{-1}$ ; (b)  $\text{SiO}_2\text{NPs}$ , 0.004%; (c, d) b + BRH ( $20, 50 \mu\text{g L}^{-1}$ ); pH 9.0.

Therefore, the concentration of BRH could be determined by fluorophotometry by using  $\text{SiO}_2\text{NPs}$  as a probe.

### 3.3. TEM images and the dynamic light scattering (DLS)

The TEM images of  $\text{SiO}_2\text{NPs}$  and the  $\text{SiO}_2\text{NPs}$ –BRH aggregates are shown in Fig. 4. When the  $\text{SiO}_2\text{NPs}$  reacted with BRH under the optimal conditions, the size increased as the aggregates of the BRH and  $\text{SiO}_2\text{NPs}$  were formed. The  $\text{SiO}_2\text{NPs}$ –BRH aggregates exhibit tufted shapes as shown in Fig. 4B.

The size distribution of  $\text{SiO}_2\text{NPs}$  and  $\text{SiO}_2\text{NPs}$ –BRH aggregates were measured by the DLS in order to confirm the formation of aggregates. As shown in Fig. 4C and D, the average

diameters of the  $\text{SiO}_2\text{NPs}$  in the solution were about 136.2 nm in the absence of BRH and they were prominently increased by roughly 90 nm at the addition of BRH due aggregation occurred.

### 3.4. Effect of pH

The pH of the solution plays an important role in the interaction between the BRH and  $\text{SiO}_2\text{NPs}$ , because it affects the surface charge properties of the  $\text{SiO}_2\text{NPs}$ . Hence, the influence of the pH on  $\Delta I_F$  was studied over a wide range of pH from 6 to 11. The results are shown in Fig. 5. The maximum value of  $\Delta I_F$  was obtained at pH 9.0. Therefore, BR buffer with pH 9.0 was used for further experiments.

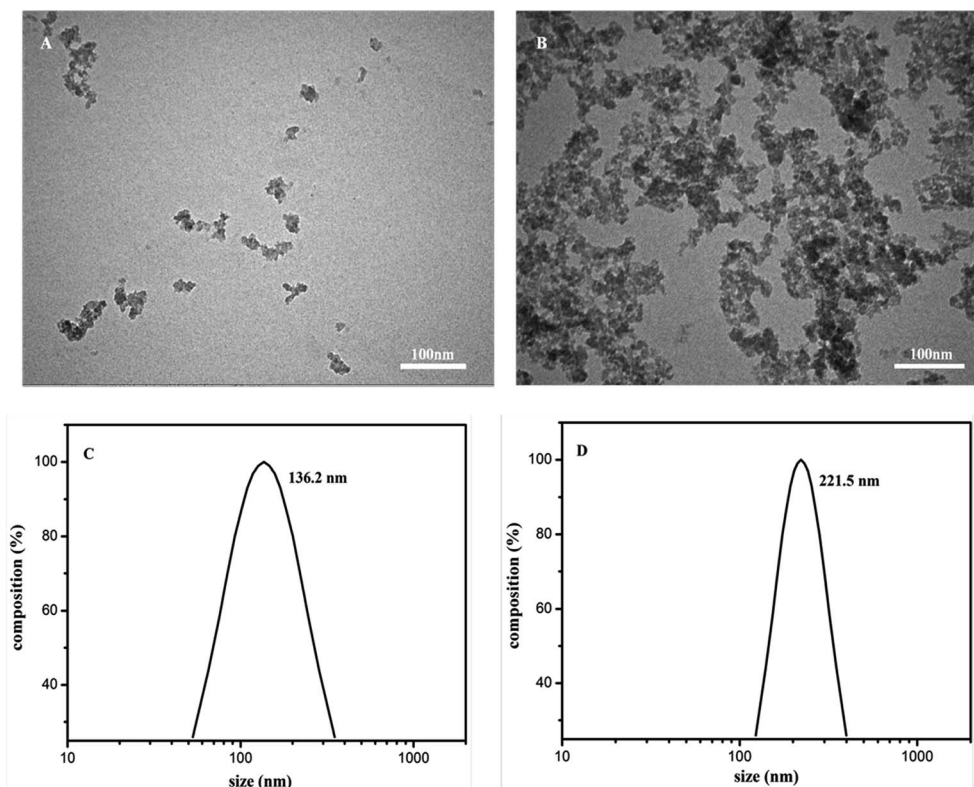


Fig. 4 TEM images of  $\text{SiO}_2\text{NPs}$  (A) and  $\text{SiO}_2\text{NPs}$ –BRH (B). The size distribution curve of  $\text{SiO}_2\text{NPs}$  (C) and  $\text{SiO}_2\text{NPs}$ –BRH (D).



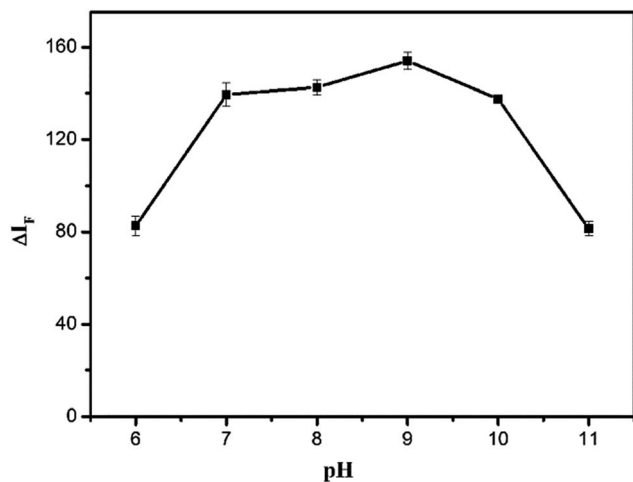


Fig. 5 Effect of pH on  $\Delta I_F$ . Conditions: SiO<sub>2</sub>NPs: 0.004%; BRH: 20.0  $\mu\text{g L}^{-1}$ .

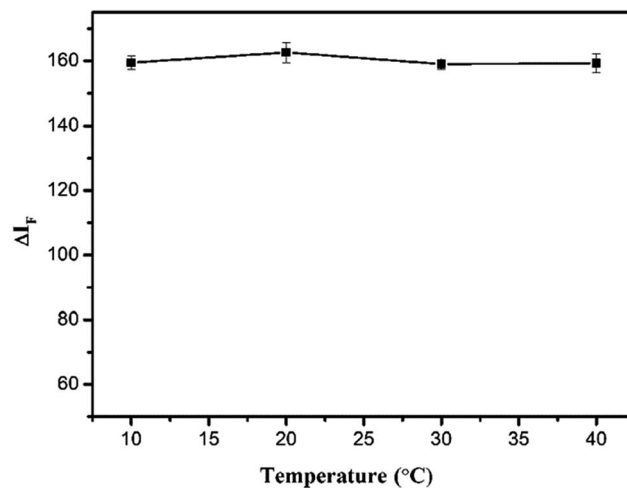


Fig. 7 Effect of reaction temperature on  $\Delta I_F$ . Conditions: SiO<sub>2</sub>NPs: 0.004%; BRH: 20.0  $\mu\text{g L}^{-1}$ ; pH 9.0.

### 3.5. Effect of reaction time and temperature

The effects of different reaction times and temperatures were investigated. As shown in Fig. 6, the  $\Delta I_F$  reached a maximum value after 30 min and remained constant for 2 h. The temperature test results (Fig. 7) indicated that the fluorescence intensity of the solution remained stable between 10 and 40 °C. Thus, 30 min of reaction time and room temperature were selected for further research.

### 3.6. Effect of concentration of SiO<sub>2</sub>NPs

The effect of the concentration of SiO<sub>2</sub>NPs on the  $\Delta I_F$  value was investigated. The linear regression equations and  $R^2$  values are given in Fig. 8. When the concentration of SiO<sub>2</sub>NPs was greater than 0.004%, the reagent blank increased and the linear range narrowed. If the concentration of SiO<sub>2</sub>NPs was lower than 0.004%, the linear range was relatively narrow because of incompleteness of the interaction between BRH and the SiO<sub>2</sub>NPs.

Therefore, 0.004% was selected as a suitable concentration for further experiments.

### 3.7. Effect of ionic strength

The influence of ionic strength on the  $\Delta I_F$  value was researched by adding different amounts of NaCl into the SiO<sub>2</sub>NPs–BRH solutions. As shown in Fig. 9, when the concentration of NaCl was lower than 150  $\text{mg L}^{-1}$ , the  $\Delta I_F$  value remained constant. By contrast, when the concentration of NaCl was higher than 150  $\text{mg L}^{-1}$ , the  $\Delta I_F$  value reduced as the concentration of NaCl increased. This could be interpreted as the shielding and competing effects of Cl<sup>−</sup> and Na<sup>+</sup> on the binding process between the BRH and SiO<sub>2</sub>NPs.

### 3.8. Effect of coexisting ions

Under the optimal experimental conditions, the interference of coexisting ions in the solution was investigated for the

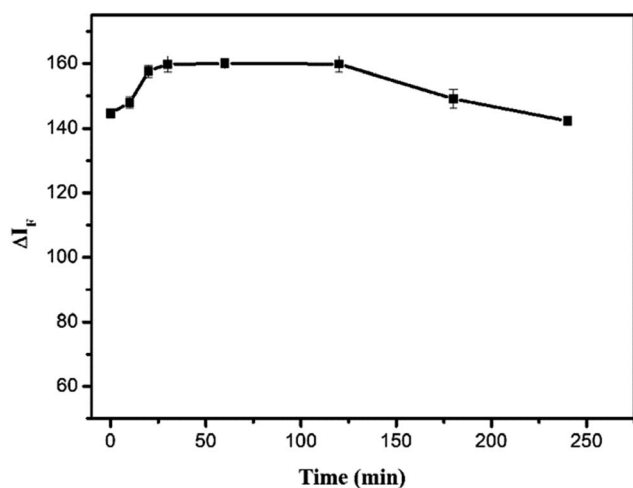


Fig. 6 Effect of reaction time on  $\Delta I_F$ . Conditions: SiO<sub>2</sub>NPs: 0.004%; BRH: 20.0  $\mu\text{g L}^{-1}$ ; pH 9.0.

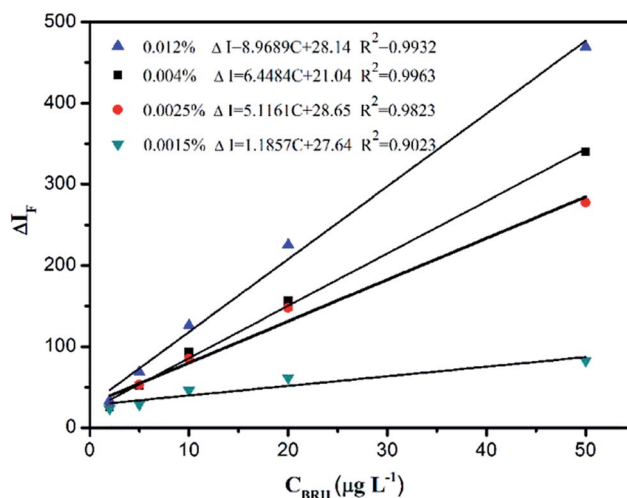


Fig. 8 Effect of SiO<sub>2</sub>NPs concentration. Conditions: pH 9.0.



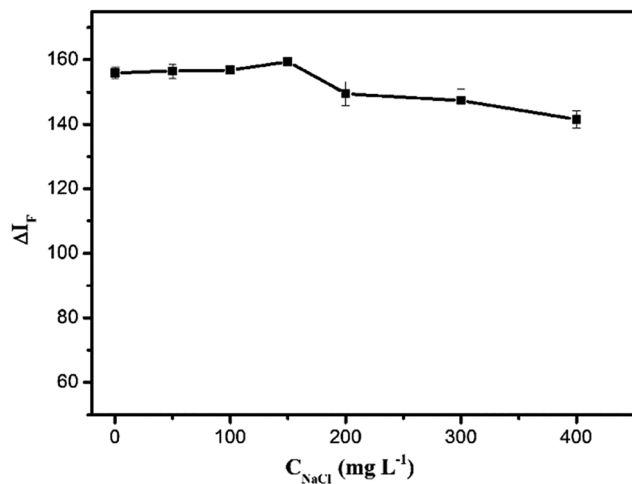


Fig. 9 Effect of ionic strength. Conditions: SiO<sub>2</sub>NPs: 0.004%; BRH: 20.0 μg L<sup>-1</sup>; pH 9.0.

determination of BRH. The experiments were carried out by fixing the concentration of BRH at 10.0 μg L<sup>-1</sup>, and then the fluorescence intensities were recorded before and after addition

of coexisting ions to the solution. The permitted relative deviation was less than ±5%. The experimental results are listed in Table 1. Most of the coexisting ions did not interfere with the determination of BRH. Only Mg<sup>2+</sup>, Ca<sup>2+</sup>, Co<sup>2+</sup>, Ni<sup>2+</sup> and Cu<sup>2+</sup> ions showed interference with the determination of BRH at low concentrations. In order to avoid interference from the metal ions, 1.0 mL of the chelating agent ethylene diamine tetraacetic acid (EDTA; 100.0 mg L<sup>-1</sup>) was added.

### 3.9. Working curve and detection limit

According to the general procedure above, when a certain amount of BRH working solution was added, the fluorescence intensities of the solution and reagent blank were measured at 540 nm with an excitation wavelength of 355 nm. As shown in Fig. 10A, the fluorescence intensity increased with an increasing concentration of BRH. There was a good linear relationship (Fig. 10B) between the ΔI<sub>F</sub> value and the concentration of BRH in the range of 2.0–50.0 μg L<sup>-1</sup>. The linear equation was ΔI<sub>F</sub> = 6.4484c + 21.04 (c in μg L<sup>-1</sup>), with R<sup>2</sup> = 0.9963. The relative standard deviation is 1.58% (n = 11). Under the optimal conditions, the limit of detection (LOD; 3σ/k) was 0.73 μg L<sup>-1</sup>.

Table 1 Interference of coexisting ions ([BRH] = 10.0 μg L<sup>-1</sup>)

Interfering ions	Concentration (mg L <sup>-1</sup> )	Relative error (%)	Interfering ions	Concentration (mg L <sup>-1</sup> )	Relative error (%)
Na <sup>+</sup>	150	5.0	Co <sup>2+</sup>	0.1, 0.4 <sup>a</sup>	1.7
K <sup>+</sup>	35	3.5	Ni <sup>2+</sup>	0.1, 0.4 <sup>a</sup>	4.1
NH <sub>4</sub> <sup>+</sup>	30	1.1	NO <sub>3</sub> <sup>-</sup>	100	3.7
Mg <sup>2+</sup>	1, 10 <sup>a</sup>	3.8	SO <sub>4</sub> <sup>2-</sup>	100	-2.9
Ca <sup>2+</sup>	1.5, 10 <sup>a</sup>	2.2	Cl <sup>-</sup>	150	5.0
Cu <sup>2+</sup>	0.02, 3 <sup>a</sup>	2.1	SiO <sub>3</sub> <sup>2-</sup>	30	4.2
Zn <sup>2+</sup>	0.05	2.4	Sucrose	300	3.1
Mn <sup>2+</sup>	0.8	2.6	Glucose	200	-1.0
Al <sup>3+</sup>	0.8	3.2	Tragantine	80	-1.9
Fe <sup>3+</sup>	1	4.7	Urea	8	5.0
Fe <sup>2+</sup>	1	1.7			

<sup>a</sup> The acceptable concentration of coexisting ions after addition of EDTA.

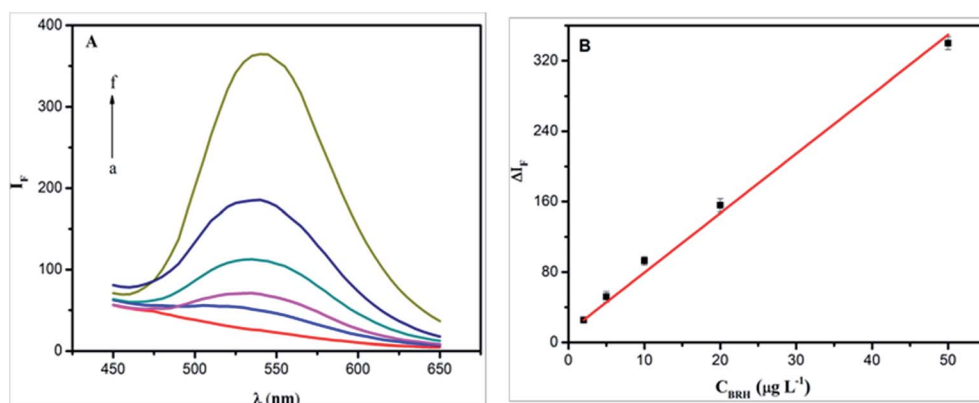


Fig. 10 The fluorescence spectra of SiO<sub>2</sub>NPs-BRH (A) and calibration curve for determination of BRH (B). Conditions: SiO<sub>2</sub>NPs: 0.004%; BRH: (a–f): 0, 2.0, 5.0, 10.0, 20.0, and 50.0 μg L<sup>-1</sup>; pH 9.0.





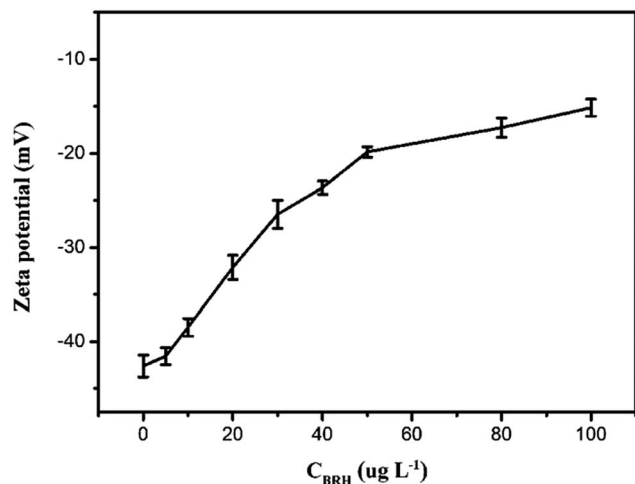


Fig. 11 Zeta potential curve of SiO<sub>2</sub>NPs–BRH. Conditions: SiO<sub>2</sub>NPs: 0.004%; BRH: 0, 5.0, 10.0, 20.0, 30.0, 40.0, 50.0, 80.0 and 100.0 μg L<sup>-1</sup>; pH 9.0.

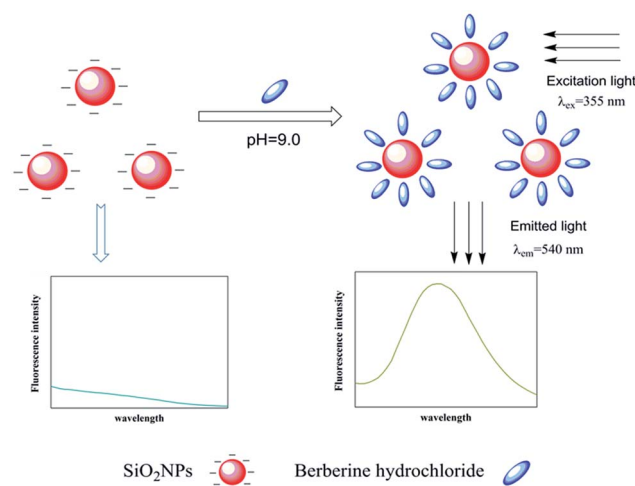


Fig. 12 Schematic illustration of the possible procedure for the detection of BRH.

### 3.10. Mechanism of reaction

It is well known that BRH is almost nonfluorescent in water, the nonfluorescent behaviour could either due to low lying intra-molecular charge transfer state or vibrational coupling of excited state with water molecules, but it fluoresces appreciably when it is dissolved in some organic solvents, or incorporated in cyclodextrins,<sup>25,26</sup> calixarenes,<sup>27</sup> and cucurbits.<sup>38</sup> In the paper, it was found that the fluorescence intensity of BRH was increased in aqueous media with SiO<sub>2</sub>NPs. In order to further investigate interaction between SiO<sub>2</sub>NPs and BRH, the zeta potential of the SiO<sub>2</sub>NPs–BRH solution was measured and the results were shown in Fig. 11. The zeta potential of the SiO<sub>2</sub>NPs was –42.6 mV because of dissociation of silicon hydroxyl on the surface. The zeta potential move gradually toward zero with the increase in BRH with positive charges. The binding of SiO<sub>2</sub>NPs with BRH would make the surface of SiO<sub>2</sub>NPs–BRH aggregates more hydrophobic. The results indicated that the aggregation of SiO<sub>2</sub>NPs–BRH was the neutralization of charges upon electrostatic interaction and increase of hydrophobicity. The marked enhancement of fluorescence intensity is due to aggregation induced emission enhancement.<sup>39–41</sup> A schematic diagram of the possible procedure is presented in Fig. 12.

## 4. Application

To demonstrate the viability of this method, the developed procedure was used for the determination of BRH in real samples. The reliability and accuracy of the method was proved by recovery tests. The determination of each sample was conducted six times in parallel. The recoveries were between 97.06 and 101.6%. The determination results were compared with the results from the pharmaceutical method<sup>42</sup> through a *t*-test analysis. There was no significant difference between the proposed and standard method under the confidence level of 95%. The results are shown in Table 2.

In addition, this method was also compared with previous methods for BRH determination. The comparison is given in Table 3 and indicates that this method has better sensitivity than most other methods.

Table 2 Results of determination of BRH in tablets (*n* = 6)

Sample	Added (μg L <sup>-1</sup> )	Found <sup>a</sup> (μg L <sup>-1</sup> )	Recovery (%)	Pharmaceutical method (mg per piece)	This method (mg per piece)	<i>t</i> -Test <i>t</i> <sub>0.05,5</sub> = 2.57
1 <sup>b</sup>	0	18.71 ± 0.309	—	99.50	100.4 ± 1.66	1.35
	10.0	28.54 ± 0.260	98.27 ± 2.60	—	—	—
	15.0	33.27 ± 0.541	97.06 ± 3.60	—	—	—
2 <sup>c</sup>	0	14.39 ± 0.298	—	49.33	50.38 ± 1.04	2.46
	10.0	24.42 ± 0.258	100.3 ± 3.33	—	—	—
	15.0	29.63 ± 0.514	101.6 ± 3.43	—	—	—
3 <sup>d</sup>	0	17.06 ± 0.541	—	34.88	34.40 ± 1.09	1.09
	10.0	27.20 ± 0.559	101.4 ± 5.54	—	—	—
	15.0	31.75 ± 0.545	97.94 ± 3.64	—	—	—

<sup>a</sup> Mean ± standard deviation (*n* = 6). <sup>b</sup> Berberine hydrochloride tablets, Chengdu Jinhua Pharmaceutical Co., Ltd. (Chengdu, China). <sup>c</sup> Compound ancklandia and berberine tablets, Grand Pharmaceutical Huangshi Feiyun Pharmaceutical Co., Ltd. (Hubei, China). <sup>d</sup> Amaranth berberine capsule, Fuzhou Neptunus Jinxiang Chinese Medicine Pharmaceutical Co., Ltd. (Fuzhou, China).



**Table 3** Comparison of this work with some of other reported methods for BRH determination

Method	Probe	LDR <sup>e</sup> ( $\mu\text{g L}^{-1}$ )	LOD ( $\mu\text{g L}^{-1}$ )	Ref.
UV <sup>a</sup>	—	118–706.0	—	6
UV	AuNPs	240–860	60	8
HPLC	—	50–5.0 $\times 10^4$	10	13
RRS <sup>b</sup>	AuNPs	1.33–240.0	0.40	10
CE <sup>c</sup>	Cyclodextrin	100–13.4 $\times 10^3$	15.7	14
EC <sup>d</sup>	—	58.8–7.06 $\times 10^3$	32.9	15
Fluorescence	Cucurbit[7]uril	3.20–2.00 $\times 10^3$	1.1	28
Fluorescence	Cucurbit[7]uril	7.43–11.2 $\times 10^3$	4.2	38
Fluorescence	Cyclodextrin	12.8–1.00 $\times 10^4$	3.6	25
Fluorescence	Cyclodextrin	94.1–4.71 $\times 10^3$	11.8	26
Fluorescence	SiO <sub>2</sub> NPs	2.0–50.0	0.73	This work

<sup>a</sup> Ultraviolet absorption. <sup>b</sup> Resonance Rayleigh scattering. <sup>c</sup> Capillary electrophoresis. <sup>d</sup> Electrochemical analysis. <sup>e</sup> Linear dynamic range.

## 5. Conclusions

This paper describes the development of a simple and novel fluorimetric method based on the increase in the fluorescence intensity of BRH after addition of SiO<sub>2</sub>NPs. The mechanism of the enhancement of fluorescence intensity has been discussed and the effects of the key experimental parameters on the fluorescence enhancement have also been described in detail. The proposed method allows the direct determination of BRH in aqueous solution with good accuracy, sensitivity, and tolerance. The amount of BRH can be measured without any complicated or time-consuming sample pretreatment processes. Compared with other reported methods, the proposed method is more sensitive, rapid, and environmentally friendly. This method was used for the detection of BRH in actual samples with satisfactory results.

## Conflicts of interest

There are no conflicts of interest to declare.

## References

- S. Bandyopadhyay, P. H. Patra, A. Mahanti, D. K. Mondal, P. Dandapat, S. Bandyopadhyay, I. Samanta, C. Lodh, A. K. Bera, D. Bhattacharyya, M. Sarkar and K. K. Baruah, *Asian Pac. J. Trop. Med.*, 2013, **6**, 315–319.
- R. Gautam and S. M. Jachak, *Med. Res. Rev.*, 2009, **29**, 767–820.
- L. M. Xia and M. H. Luo, *Chronic Dis. Transl. Med.*, 2015, **1**, 231–235.
- C. M. Tian, X. Jiang, X. X. OuYang, Y. O. Zhang and W. D. Xie, *Chin. J. Nat. Med.*, 2016, **14**, 518–526.
- H. P. Kuo, T. C. Chuang, M. H. Yeh, S. C. Hsu, T. D. Way, P. Y. Chen, S. S. Wang, Y. H. Chang, M. C. Kao and J. Y. Liu, *J. Agric. Food Chem.*, 2011, **59**, 8216–8224.
- T. Sakai, *Analyst*, 1983, **108**, 608–614.
- T. Sakai, *Analyst*, 1991, **116**, 187–190.
- Z. W. Hu, M. S. Xie, D. T. Yang, D. Chen, J. Y. Jian, H. B. Li, K. S. Yuan, Z. J. Jiang and H. B. Zhou, *RSC Adv.*, 2017, **7**, 34746–34754.
- X. B. Pang and C. Z. Huang, *J. Pharm. Biomed. Anal.*, 2004, **35**, 185–191.
- S. P. Liu, Z. Yang, Z. F. Liu, J. T. Liu and Y. Shi, *Anal. Chim. Acta*, 2006, **572**, 283–289.
- P. Biparva, S. M. Abedirad, S. Y. Kazemi and M. Shanehsaz, *Sens. Actuators, B*, 2016, **234**, 278–285.
- G. H. Liu, W. He, H. Cai, X. M. Sun, W. E. Hou, M. N. Lin, Z. Y. Xie and Q. F. Liao, *Anal. Methods*, 2014, **6**, 2998–3008.
- P. L. Tsai and T. H. Tsai, *J. Chromatogr. A*, 2002, **961**, 125–130.
- S. Uzasci and F. B. Erim, *J. Chromatogr. A*, 2014, **1338**, 184–187.
- A. Geto, M. Pita, A. L. De Lacey, M. Tessema and S. Admassie, *Sens. Actuators, B*, 2013, **183**, 96–101.
- J. F. Song, Y. Y. He and W. Guo, *J. Pharm. Biomed. Anal.*, 2002, **28**, 355–363.
- H. M. Al-Saidi and M. S. El-Shahawi, *Spectrochim. Acta, Part A*, 2015, **138**, 736–742.
- J. R. Bi, H. T. Wang, T. Kamal, B. W. Zhu and M. Q. Tan, *RSC Adv.*, 2017, **7**, 30481–30487.
- G. Q. Gong, Z. X. Zong and Y. M. Song, *Spectrochim. Acta, Part A*, 1999, **55**, 1903–1907.
- M. X. Gao, J. L. Xu, Y. F. Li and C. Z. Huang, *Anal. Methods*, 2013, **5**, 673–677.
- Y. Y. Liu, H. C. Li, B. Guo, L. J. Wei, B. Chen and Y. Y. Zhang, *Biosens. Bioelectron.*, 2017, **91**, 734–740.
- P. J. Ni, Y. J. Sun, S. Jiang, W. D. Lu, Y. L. Wang and Z. Li, *Sens. Actuators, B*, 2017, **240**, 651–656.
- X. Y. Zheng, T. M. Yao, Y. Zhu and S. Shi, *Biosens. Bioelectron.*, 2015, **66**, 103–108.
- S. Liang, Y. F. Kuang, F. F. Ma, S. Chen and Y. F. Long, *Biosens. Bioelectron.*, 2016, **85**, 758–763.
- F. Liu, H. L. Liang, K. H. Xu, L. L. Tong and B. Tang, *Talanta*, 2007, **74**, 140–145.
- Y. Yang, X. Yang, C. X. Jiao, H. F. Yang, Z. M. Liu, G. L. Shen and R. Q. Yu, *Anal. Chim. Acta*, 2004, **513**, 385–392.
- M. Megyesi and L. Biczok, *Chem. Phys. Lett.*, 2006, **424**, 71–76.
- Y. P. Li, H. Wu and L. M. Du, *Chin. Chem. Lett.*, 2009, **20**, 322–325.
- K. A. Connors, *Chem. Rev.*, 1997, **97**, 1325–1357.
- I. Miletto, A. Gilardino, P. Zamburini, S. Dalmazzo, D. Lovisollo, G. Caputo, G. Viscardi and G. Martra, *Dyes Pigm.*, 2010, **84**, 121–127.
- S. Liang, K. Shephard, D. T. Pierce and X. J. Zhao, *Nanoscale*, 2013, **5**, 9365–9373.
- A. Hemadi, A. Ekrami, H. Oormazdi, A. R. Meamar, L. Akhlaghi, A. R. Samarraf-Zadeh and E. Razmjou, *Acta Trop.*, 2015, **145**, 26–30.
- M. Qhobosheane, S. Santra, P. Zhang and W. H. Tan, *Analyst*, 2001, **126**, 1274–1278.
- K. Abnous, N. M. Danesh, A. S. Emrani, M. Ramezani and S. M. Taghdisi, *Anal. Chim. Acta*, 2016, **917**, 71–78.



- 35 A. S. Emrani, S. M. Taghdisi, N. M. Danesh, S. H. Jalalian, M. Ramezani and K. Abnous, *Anal. Methods*, 2015, **7**, 3814–3818.
- 36 J. Fan, Z. H. Xie, X. X. Teng and Y. Zhang, *Chin. Chem. Lett.*, 2017, **28**, 1104–1110.
- 37 M. Megyesi and L. Biczók, *J. Phys. Chem. B*, 2007, **111**, 5635–5639.
- 38 N. Dong, L. N. Cheng, X. L. Wang, Q. Li, C. Y. Dai and Z. Tao, *Talanta*, 2011, **84**, 684–689.
- 39 A. Gopi, A. Vindhysarumi and K. Yoosaf, *RSC Adv.*, 2015, **5**, 47813–47819.
- 40 C. J. Kassl and F. C. Pigge, *Tetrahedron Lett.*, 2014, **55**, 4810–4813.
- 41 F. Qiao, L. Zhang, Z. Lian, Z. Yuan, C. Y. Yan, S. P. Zhuo and Z. Y. Zhou, *J. Photochem. Photobiol., A*, 2017, DOI: 10.1016/j.jphotochem.2017.07.024.
- 42 The Pharmacopeia Committee of Ministry of Health PR China, *The Pharmacopeia of PR China*, China medical science Press, Beijing, 2nd edn, 2015, p. 875.

